JOURNAL OF GEOPHYSICAL RESEARCH, VOL. 90, NO. A5, PAGES 4128–4140, MAY 1, 1985

# DE 1 Observations of Siple Transmitter Signals and Associated Sidebands

K. RASTANI, U. S. INAN, AND R. A. HELLIWELL

*Space, Telecommunications, and Radioscience Laboratory, Stanford University, California*

VLF signals from the Siple Station, Antarctica, transmitter received on the DE 1 spacecraft provide new information on whistler mode signal propagation paths in the magnetosphere. In two case studies, the measured group delay in conjunction with in situ density measurements and ray tracing analysis are used to distinguish between direct nonducted propagation and a hybrid mode consisting of one-hop propagation in a duct followed after ionospheric reflection by nonducted propagation. The extent of the observations both in space and time indicates that such a hybrid propagation mode may be an important means by which whistler mode signals generated or amplified in ducts can populate the magnetosphere. Computed group time delays based on a diffusive equilibrium model for the density distribution along the field lines provide good agreement with measurements over a wide range of magnetic latitudes (50°S–25°N). In one case, observed Siple signals are associated with sidebands of ±30 Hz spacing, and emissions are occasionally triggered. Sidebands are associated with signal components that are believed to have propagated on direct nonducted paths as well as in a hybrid (ducted/nonducted) mode with the sideband spacing being equal in both cases. The sideband spacing is found to be independent of the carrier frequency and amplitude and the satellite location with respect to the magnetic equator.

## 1. INTRODUCTION

This paper reports initial results from an active wave injection experiment aimed at studying coherent VLF wave propagation and wave-particle interactions in the magnetosphere. The VLF signals were injected from the Stanford University transmitting facility at Siple Station, Antarctica (84°W, 76°S), and were received by the Stanford University linear wave receiver (LWR) on the high-altitude, polar-orbiting Dynamics Explorer 1 (DE 1) spacecraft.

The Siple/DE 1 experiments were carried out from May through August 1982 at a time when the apogee (~4.6 $R_E$) of the DE 1 orbit was within ±20° of the geomagnetic equator. Continuous observations of 1–3 hours per day at points up to ~40° away from the magnetic field lines of Siple Station were possible. Continuous ground observations were also made at Roberval, Canada (72.3°W, 48.4°N, conjugate to Siple), and Palmer, Antarctica (65°W, 65°S).

In this paper, we report on the detailed analysis of data from two days, namely May 24 and August 17, 1982. These days were selected on the basis of a preliminary observation of most of the data for the 4-month period. The May 24 case was chosen since the transmitter signals were detectable over a relatively long period. The August 17 case was selected mainly because of the observation of sidebands associated with the transmitter signals but also because of the long duration of detectable signal. In addition, as seen from Figure 1, the orbital configurations for these two days are complementary in terms of their relationship with the transmitter location.

The Siple/DE 1 VLF wave injection experiments have evolved from previous satellite (OGO's, IMP 6, Explorer 45, ISEE 1, and EXOS-B) observations of signals from various ground transmitters including the experimental transmitter at Siple Station, Antarctica [*Inan et al.*, 1977; *Bell et al.*, 1981, 1983]. The nearly field-aligned polar orbit of the DE 1 satellite and the availability of both electric and magnetic antennas have provided opportunities to survey in time and space the distribution of Siple signals within the magnetosphere.

While the earlier studies have discussed the signal characteristics and identified the propagation paths using density models derived mainly from ground-based whistler data, in this paper we analyze the propagation paths quantitatively using in situ density measurements as well as ground-based data. The long extent of continuous observations (up to ~3 hours) of the transmitter signal on the ground and on the satellite allows the probing of the magnetosphere on a wider spatial and temporal scale than in earlier cases. We also apply our results to the interpretation of sidebands associated with nonducted whistler mode signals observed near the magnetic equator on a particular pass. Some of the results given in this paper were previously reported in preliminary form [*Inan et al.*, 1982].

In the next section we describe the data received on the satellite and discuss measurements of the propagation delay, signal amplitude, and in situ electron densities. In the following two sections, ray propagation paths to the satellite for the two days of May 24 and August 17, 1982, are discussed. This is followed by the presentation of sidebands associated with Siple signals observed on August 17, 1982.

## 2. DESCRIPTION OF THE EXPERIMENT AND DATA SOURCES

Figure 1 shows the meridional plane projection of the orbital tracks of DE 1 for May 24 and August 17, 1982, during the periods 2110–0040 UT and 1530–1936 UT, respectively. The geographic longitudes at the beginning and end of both



Paper number 4A8233.
0148-0227/85/004A-8233$05.00

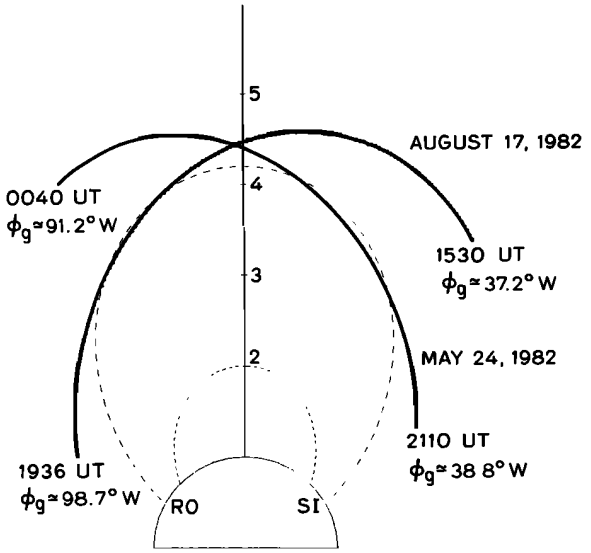


Fig. 1. Projections of DE 1 orbits onto the Siple-Roberval meridian during 2110–0040 UT on May 24, 1982, and 1530–1960 UT on August 17, 1982. The geographic longitudes at the beginning and end of the periods are indicated.

periods are indicated on the figure. A range of ~55°, more or less centered around the Siple magnetic longitude, is covered in both cases. Throughout these periods, VLF signals were transmitted continuously from Siple Station except for short breaks for frequency changes. The format of the transmissions included a series of pulses and frequency ramps of varying duration and frequency (see Figure 2) designed to study different aspects of wave propagation and wave-particle interactions. The transmitter signals were received on the satellite using the Stanford University linear wave receiver (LWR) connected to either the magnetic loop (B) or the long electric dipole ($E_x$) antennas. Description of the DE 1 wave receiver instrumentation is given elsewhere [*Shawhan et al.*, 1981; *Inan and Helliwell*, 1982].

In the two cases studied, transmitter signals were also simultaneously received at Roberval, Canada, located magnetically conjugate to Siple Station. On one day, May 24, 1982, Siple signals were clearly detectable at Roberval during the period 2250–0030 UT, while on the other day, August 17, 1982, the transmitter signals at Roberval were barely detectable, mainly because of a relatively high atmospheric noise background.

An example of the simultaneous reception of signals on the satellite and at Roberval is shown in Figure 2. The lower panel shows the frequency-time format of transmissions, the middle panel the wave spectra observed on DE 1 using the B antenna, and the upper panel the spectra received at Roberval. The three panels are aligned in absolute time, so that the group delay of the signal components from the source to the satellite and subsequently to the ground can be seen. We note here that the signals were detectable on the satellite at different $L$ shells for a duration of ~ 3 hours, which suggests propagation over nonducted paths.

The top panel of Figure 2 shows two distinct traces for each frequency ramp, indicating the presence of at least two ducts with slightly different time delays. Both of the two principal signals appear to have undergone amplification and to have triggered emissions. The satellite data also indicate the presence of an "echo" (labeled A′) that arrives at the satellite ~1.5 s after the first signal, presumably after reflecting from the ionosphere in the northern hemisphere. This hypothesis is confirmed by the analysis that follows.

### 2.1. Measurement of Group Time Delay

The measured group time delays of the Siple signals observed at the satellite are plotted in Figure 3*a* for the May 24, 1982, case. Different symbols are used to represent various transmitted frequencies, with the open symbols representing the first detectable signals having the shortest path delay and the solid symbols showing the measured delay for the later arriving signals. The continuous lines are the computed values for direct propagation, while the dashed line applies to ionospherically reflected rays, as will be discussed later. Figure 3*a* shows a steady increase in the group delay of the direct signals as the satellite moves northward (see Figure 1), while at the same time the delays of the echoes decrease. The reduction in the number of measured points at the later times is due to reduced signal levels, which rendered difficult the visual identification of pulse onset times from spectrograms.

Group delays measured along the orbit for August 17, 1982, are shown in Figure 3*b*. There are three different groups of signals, labeled with different symbols, which are presumed to have propagated in different modes as discussed later. Data in the lower portion of the figure clearly show an increase in delay as the satellite moved northward. The error bars shown in Figure 3 include the effects of uncertainty in identification of the onset of the pulses and the finite risetime (~100 ms) of the filter used for the spectrum analysis.

### 2.2. Signal Amplitudes

While the main purpose of this paper is the identification of the signal propagation paths, the data from the two days also enabled us to measure the absolute wave electric and magnetic intensities of the Siple signals. Measured wave intensities for May 24 and August 17, 1982, along with estimated values of the refractive index and comparison with expected wave signal levels are given in the appendix. The absolute wave magnetic intensities of May 24, 1982, are compared to previously reported measurements of the magnetic field component of Siple transmitter signals [*Inan et al.*, 1977] received aboard the IMP 6 satellite on June 28, 1973. To facilitate this, we selected a DE 1 orbital location similar to that of the IMP 6 case. The theoretically estimated magnetic field intensity for May 24, 1982 (see the appendix), was ~0.03 pT, in good agreement with the value of ~0.056 pT measured at ~2300 UT. However, these values are a factor of ~10 smaller than the measured intensities for June 28, 1973. This is attributed to differences in the raypath distribution for the two cases, as discussed in the appendix.

### 2.3. Background Cold Plasma Distribution

In order to model the magnetospheric cold plasma distribution for the ray path analysis we use data from three different sources. For in situ measurements of density we use results derived from upper hybrid resonance (UHR) noise bands [*Mosier et al.*, 1973; *Persoon et al.*, 1983] recorded by the University of Iowa sweep frequency receiver (SFR) instrument.

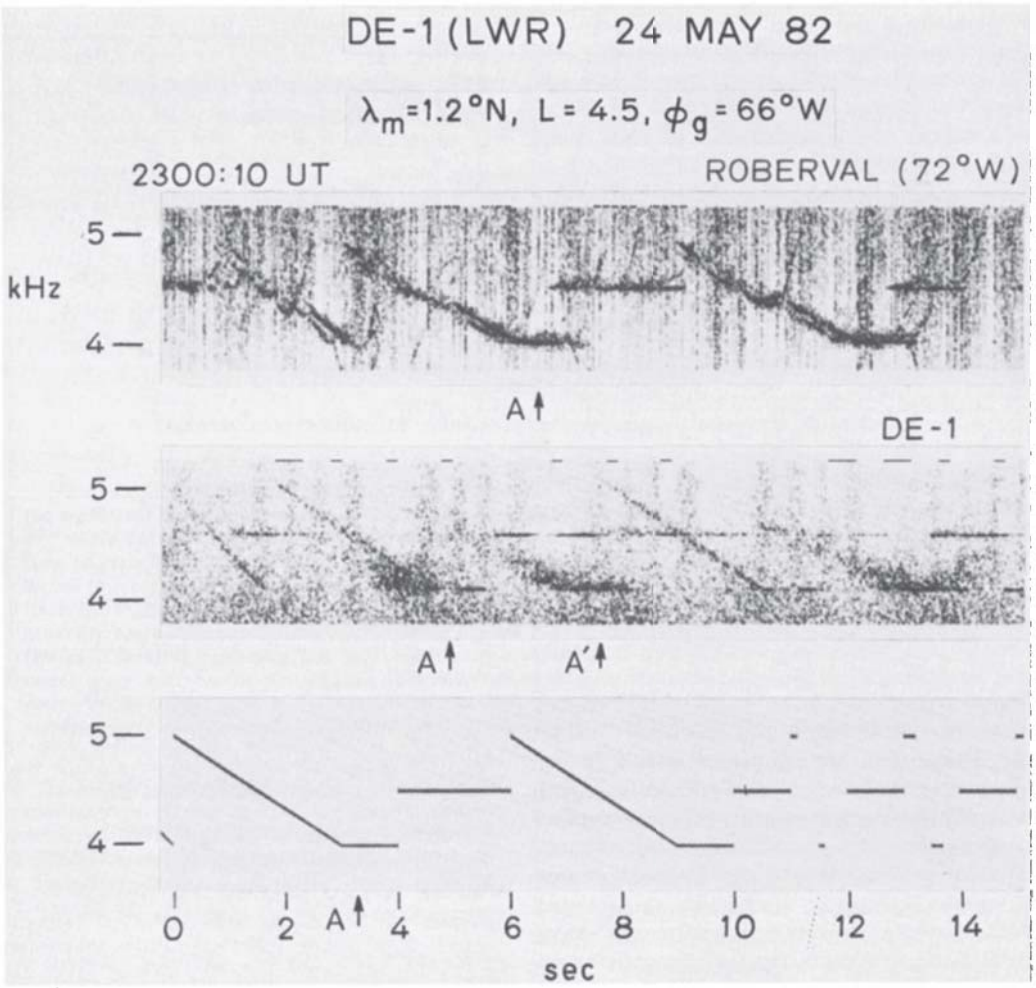


Fig. 2. Siple signals as observed on the DE 1 satellite on May 24, 1982, shown on the middle panel, with the signals observed at Roberval Station, Canada, shown in the top panel. Echoes arriving at the satellite ~1.5 s later than those on the first path are also visible in the middle panel. The Roberval data reveal two distinct paths of propagations at different $L$ shells. The lower panel shows the format of the transmitted signals. The three panels are aligned in absolute time so that the group time delay can be seen. To aid this comparison, a representative signal element is labeled with an A on each panel, a satellite echo of this signal is labeled A'.

In order to be comparable with the densities derived from other techniques discussed below and also to be readily usable in an existing ray-tracing code, in situ densities are mapped onto a meridional plane. They are then transformed to the magnetic equator by means of a diffusive equilibrium model of the density distribution along the field lines [*Angerami and Thomas*, 1964]. The resulting equatorial densities are shown with solid circles in Figures 4*a* and 4*b* for May 24, and August 17, 1982, respectively.

A second source of information on cold plasma density on May 24, 1982, is the broadband VLF data acquired at Palmer Station, Antarctica. A dispersion analysis [*Park*, 1972] carried out on a number of whistler components received at Palmer during 2255–2256 UT results in equatorial cold plasma density values as a function of $L$ shell of propagation, as shown with crosses in Figure 4*a*.

A third source of density information is the dispersion as observed at Roberval of Siple signals themselves. Over the period 2251–0030 UT on May 24, 1982, the center frequency of Siple transmissions was varied from 4.57 to 2.05 kHz, and signals were continuously observed at Roberval. Assuming that the propagation path (whistler mode duct) remained stable during this period, group time delays of Siple signals at different frequencies are measured in order to define the frequency-time dispersion at the $L$ shell of propagation. The result is shown in Figure 5. Analysis of this "synthesized whistler" trace provide estimates of $L$=4.25±0.1 for the propagation path and $n_{eq}$=470±20 el/cm$^3$ for the equatorial cold plasma density.

## 3. Case 1: May 24, 1982

To determine the ray propagation paths we use the Stanford University VLF ray-tracing program [*Burtis*, 1973; *Inan and Bell*, 1977]. An equatorial density distribution that is believed to be representative of the in situ densities is shown by the solid curve in Figure 4*a*. This profile is also in general agreement with the fact that the geomagnetic conditions were relatively quiet on May 24, 1982 and on several preceding days. Sample 4.8 kHz ray paths for this profile showing multiple rays injected at different locations are given in Figure 6*a*. Those chosen for illustration are injected at 630 km altitude at magnetic latitudes of 64.7°S–65.1°S with wave normals initially along the local vertical. The computed

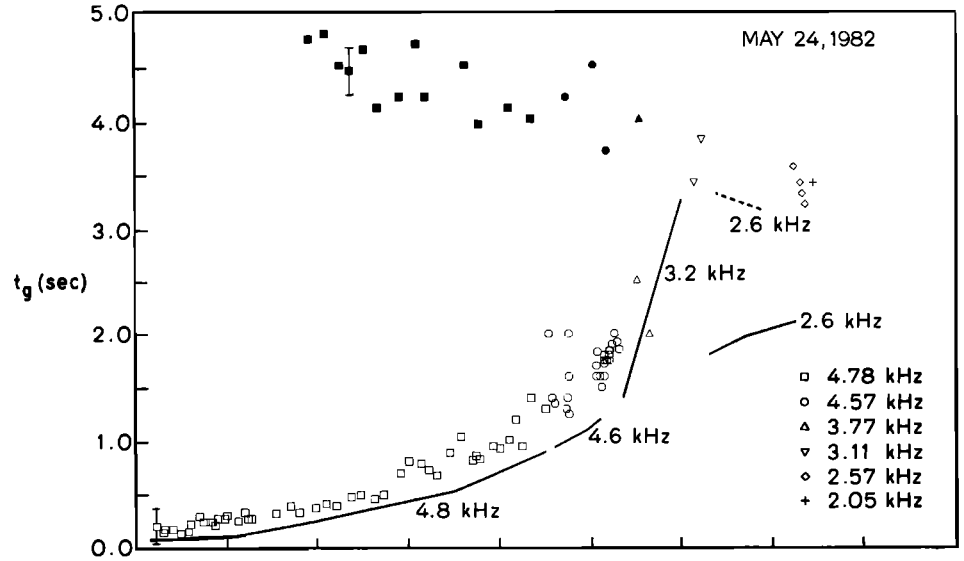


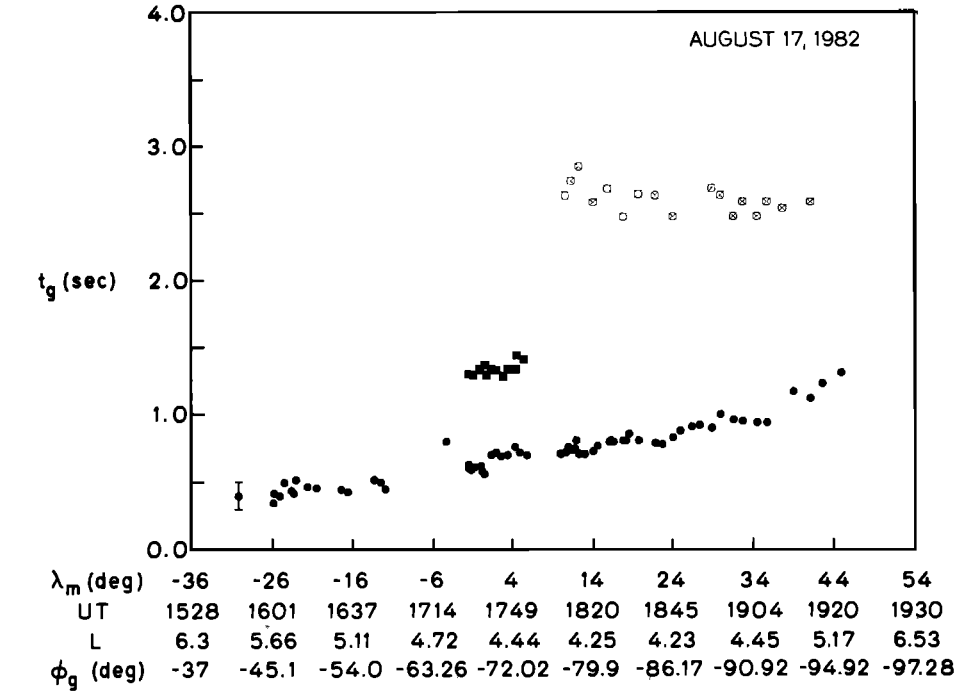


Fig. 3. (*a*) The measured time delays of Siple signals on DE 1 for May 24, 1982, 2113–0020 UT. Different symbols correspond to different transmitter frequencies. The solid symbols identify the delays for the echoes and open symbols for the direct signals. The solid lines show the group delays computed for different frequencies using ray tracing on a direct path. The dashed line shows computed values for ionospherically reflected rays at 2.6 kHz. (*b*) Group time delays measured on August 17, 1982, during 1528–1920 UT. Different symbols represent different modes of propagation that are discussed in the text. The error bars in both figures represent errors due to identification of pulse onset time and also the analysis filter risetime.

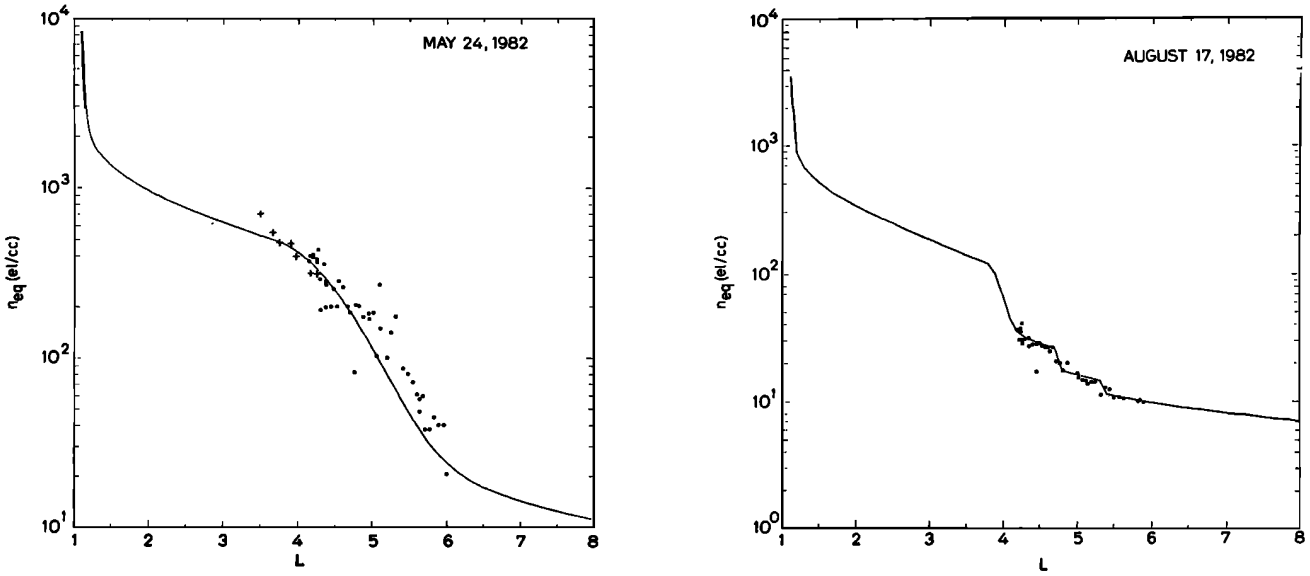


Fig. 4. (*a*) The solid line shows the equatorial cold plasma density distribution used for the raypath analysis of the data for May 24, 1982. The dots are the equatorial mappings of the in situ measured densities. The crosses are the equatorial densities obtained from whistlers observed at Palmer Station and the density obtained from the "synthesized whistler" of Figure 5. (*b*) A structured equatorial cold plasma density distribution for August 17, 1982, with the dots being the equatorial projections of the measured in situ density values.

group time delays from the injection point up to the point of intersection of the ray with the satellite orbital track are shown by the solid lines in Figure 3*a*. These represent the delays for direct propagation paths and in terms of variation with time are in relatively good agreement with the measured delays up to ~2300 UT. The fact that the computed delays are consistently lower than the measured ones may in part be due to the telemetry delay for the transmission of the satellite data to the ground station. This delay is estimated to be 60-70 ms and is not accounted for in the results shown in Figure 3*a*. The relatively sharp increase in the computed group delay after this time is due to the inward bending of the ray paths for 3.2 kHz which makes the satellite locatin increasingly less accessible as the spacecraft moves past the equator. Note that lower-frequency rays (2.6 kHz) curve inward at higher $L$ shells; thus the satellite locations are more accessible and with lower time delays.

As mentioned above, the open symbols in Figure 3*a* represent the group delay for the first arriving signal components, whereas the solid symbols are the time delays for the later arriving signals (i.e., echoes). The time delays of the echoes shown with solid symbols in Figure 3*a* decrease with time as the satellite moves toward and past the equator and away from the transmitter. This suggests that the echo signals may have resulted from reflections in the northern hemisphere of one-hop ducted signals. Such a ducted/nonducted propagation mode can be referred to as a "hybrid" propagation mode and has been previously suggested for interpretation of observation of man-made and natural VLF signals observed on satellites [*Bell et al.*, 1983; *Smith et al.*, 1984].

The measured propagation delays of the first observable 2.6 kHz signals in Figure 3*a* (near 0020 UT) do not agree with those computed on the basis of direct nonducted propagation (solid line). This suggests that these signals also represent ionospheric reflections of one-hop ducted signals and are identified as the first arriving signal components since the direct nonducted signals do not reach the satellite for times after ~2330 UT. The fact that the satellite longitude at this time is very close to that of the Siple/Roberval field lines indicates that these signals may be the reflected components of the same ducted signals observed at the conjugate station Roberval, Canada. These signals arrive at the satellite following reflection and subsequent upward propagation in a nonducted mode [*Bell et al.*, 1983]. To demonstrate this, 2.6 kHz rays were injected at various locations in the north and with different wave normal angles using the density profile of Figure 4*a*. Rays injected at 630 km and at a latitude of 63°N with wave normals in the range 9.8°–10.1° with respect to the vertical were found to reach the satellite locations corresponding to times after 2341 UT. These rays are plotted in Figure 6*b*.

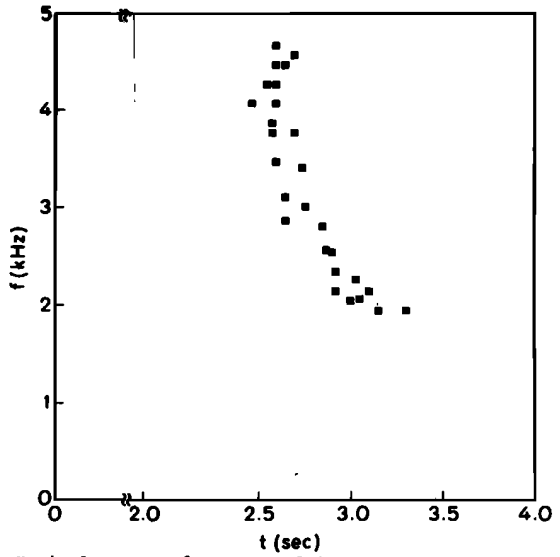


Fig. 5. A plot versus frequency of the group delays Siple pulses observed at Roberval during 2251–0030 UT on May 24, 1982, forming a "synthesized whistler."

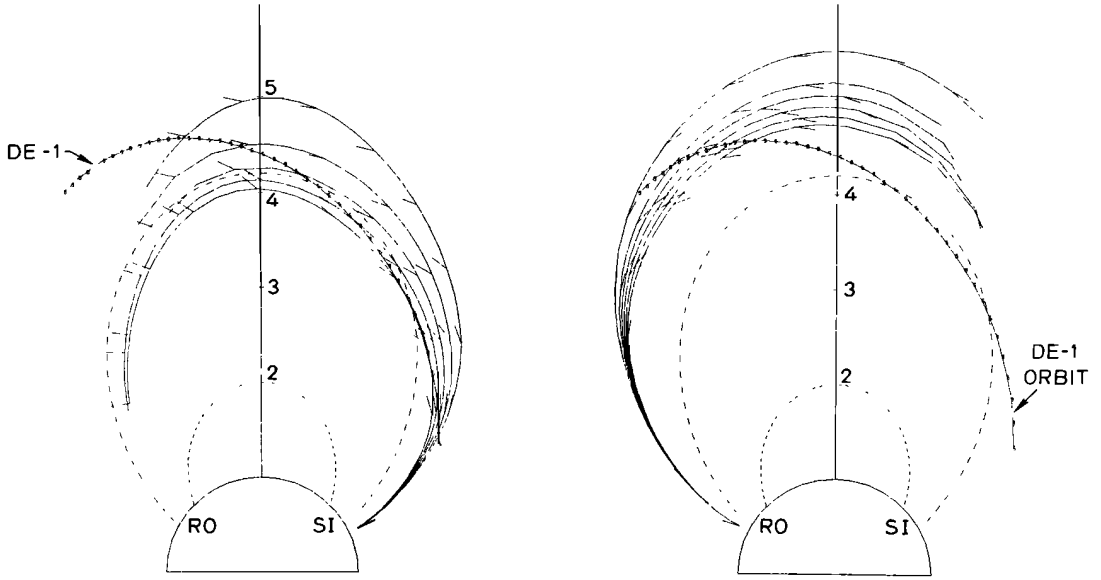


Fig. 6. (*a*) Nonducted 4.8 kHz rays injected vertically into the plasma density distribution represented in Figure 4*a* a magnetic latitudes 64.7°–65.1°S and 630 km altitude. The short line segments on the ray path show the wave normal angles along the ray path. The satellite path for the May 24, 1982, case is shown as the beaded line. (*b*) Nonducted 2.6 kHz rays injected in the northern hemisphere with wave normals varying between 9.8°and 10.1°, representing rays reflected from the ionosphere.

The total group delay of these reflected rays must consist of the delay in the ducted mode from the transmitter to Roberval (~2.6 s for the earliest path) plus the subsequent delay from the reflection point in the ionosphere to the satellite. The computed result is plotted with a dashed line in Figure 3*a* and agrees reasonably well with the variations of the data points.

While the ray tracing applied on a diffusive equilibrium model seems to simulate the measurements as shown in Figure 3, the question of the uniqueness of the ray paths needs to be discussed. In a two-dimensional ray-tracing model as considered here, the ray paths to the satellite location from any given injection point in the ionosphere are dependent on initial wave normal angle. Rays entering the ionosphere at different latitudes can also arrive at the satellite location depending on the gradients of the cold plasma density. This would especially be the case when irregularities are present in the ionosphere through which the waves would travel. However, in a smooth model of the cold plasma distribution as considered here, waves arriving to the satellite over different paths would be expected to have measurably different time delays. In that sense, we can view the ray paths discussed as being unique in that the group time delay over other ray paths would not, in general, be in agreement with the data.

The results of Figure 3*a* show general agreement between computed and measured group time delays. This finding validates the use of diffusive equilibrium models of cold plasma along the field lines, this model having been used both for the mapping of density values and for the ray-tracing calculations. Our results therefore support earlier comparisons of in situ densities with those obtained from ground-based whistler data [*Carpenter et al.*, 1981] and also extend these results, since agreement between model and data is maintained over a large span of time and space and in regions well away from the equator for which ground-observed whistlers form only a rough integral method of measurements.

## 4. Case 2: August 17, 1982

Examples of Siple transmitter signals received on DE 1 during August 17, 1982 are shown in Figure 7. The transmission format, similar to the May 24, 1982, case, is illustrated in the second and fourth panels, located below the corresponding dynamic spectra. The data and the format panels are aligned in absolute time so that the propagation delay from the time of initiation of the signals to the time they first appear at the satellite can be seen.

The data show the presence of at least two distinct paths with a time delay difference of ~0.6 s as evidenced by the double frequency-ramp components and the extended durations of the constant frequency pulses. The transmitter signals are apparently associated with sideband components (spacing ~±30 Hz) and occasionally with triggered rising emissions, to be discussed in the next section; in this section we concentrate on the signal propagation modes.

During the period 1600–1800 UT on August 17, 1982, Siple transmitter signals were also observed at the conjugate point Roberval, Canada. However, the existence of a very high level of background atmospherics precluded accurate measurements of these signals.

To study the propagation paths for this case, the same procedure as for case 1 is employed. Magnetic conditions on this day and the few preceding days were also relatively quiet. An equatorial density profile that is in approximate agreement with in situ densities is modeled as shown with the solid line of Figure 4*b*. This profile contains fine structure that was not present for case 1 (Figure 4*a*). Sharp density gradients, visible in Figure 4*b*, can provide guiding for the rays much like secondary plasmapauses [*Inan and Bell*, 1977; *Gorney and Thorne*, 1980]. Figure 8*a* shows raypaths of 4.1-kHz signals injected at 630 km altitude with vertical wave normal angles. Rays are guided by one of the sharp gradients located at $L \simeq 5.4$ as indicated by the outermost dashed line in Figure 8*a* and are nearly field aligned until

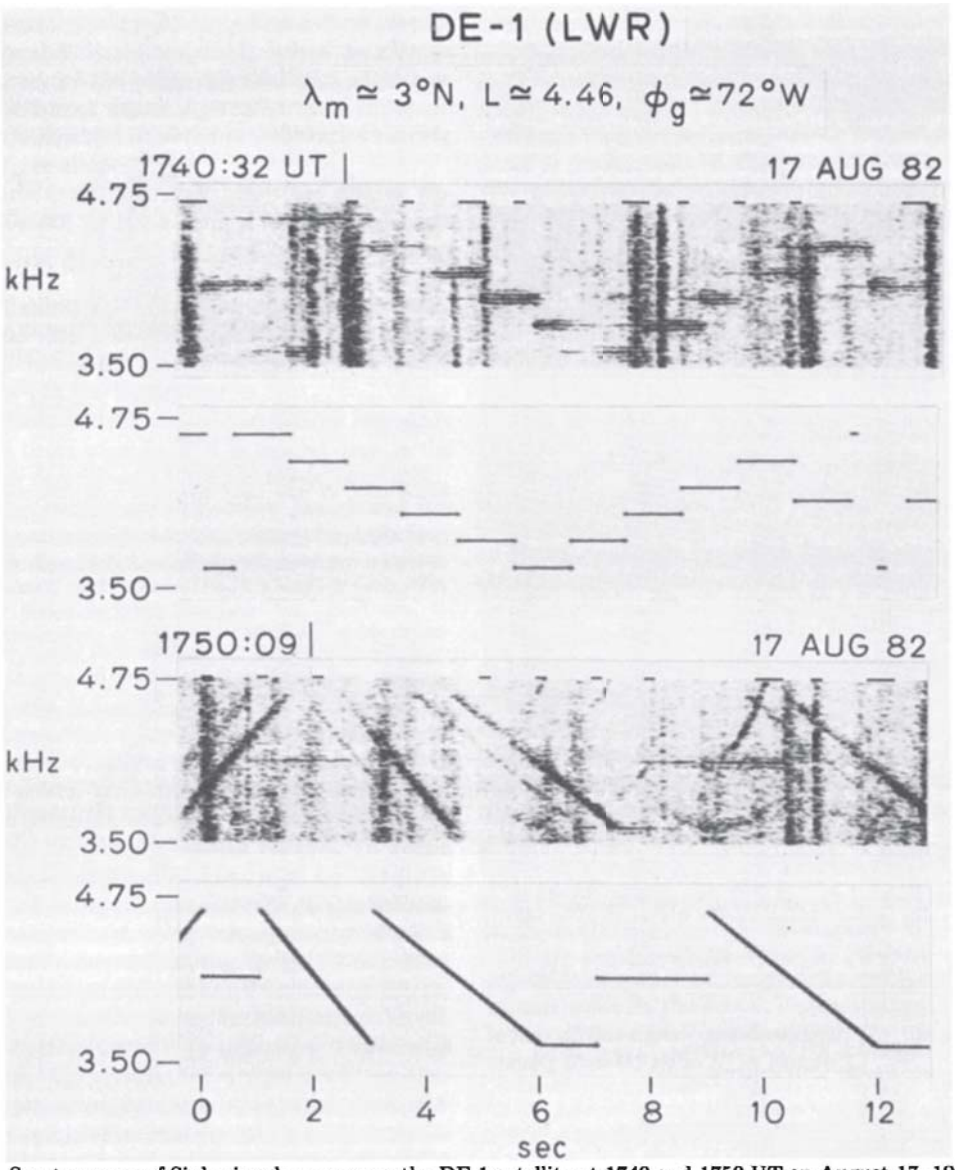


Fig. 7. Spectrograms of Siple signals as seen on the DE 1 satellite at 1740 and 1750 UT on August 17, 1982, with the transmitted format shown in the second and fourth panels. The sidebands associated with the Siple signal as well as triggered rising emissions can be seen.

they cross the satellite path. The same rays cross the satellite trajectory again at lower altitudes and in the northern hemisphere.

These rays have computed time delays that are ~30% lower than the measured values (data plotted in the lower portion of Figure 3*b*) for the southern crossings of the satellite path and time delays ~30% higher than the data for the northern crossings. This result is unlike that of case 1, in which computed time delays were consistently lower than the data, and suggests that the cold plasma density distribution for August 17, 1982, contained substantial structure in addition to that indicated in Figure 4*b*. Note that longitudinal variations in the plasma density are not accounted for in our analysis; such variations could further complicate determination of the density distribution. Since construction of a more detailed density model is not feasible using the available analysis tools and data, the analysis of the ray propagation for this case is based both on ray-tracing analysis in the density model shown in Figure 4*b* and on qualitative comparison with the results of case 1.

Figure 3*b* implies the existence of three distinct propagation modes corresponding to the three groups of data points. The group delays measured continuously along the orbit and shown as the lowest-time-delay group in Figure 3*b* are interpreted as representing direct propagation paths. They show the characteristics of the direct mode of case 1, in that (1) they correspond to signals that are continuously observed along the path and (2) the group delays increased as the satellite moved away from the source. The points corresponding to the longest delays shown on Figure 3*b* seem to decrease in time as the satellite moves to higher latitudes. This is the characteristic that we associated with ionospherically reflected rays in case 1, and suggests that these points represent propagation in a similar mode.

The third group of propagation delays, corresponding to the middle group of data points in Figure 3*b* (~1730–1800

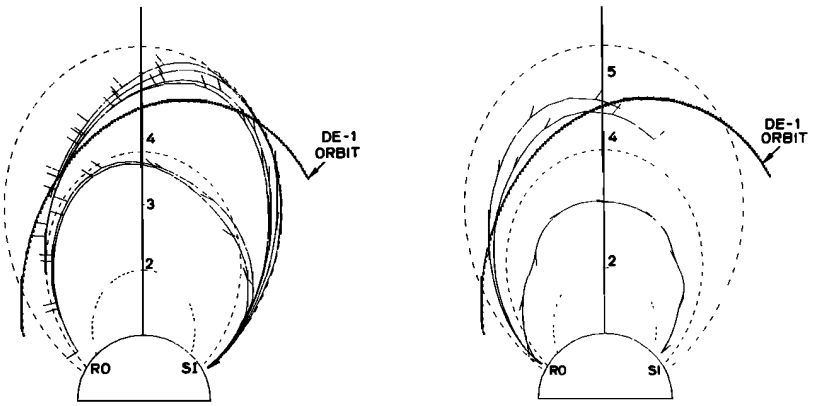


Fig. 8. (*a*) Nonducted 4.1-kHz rays injected vertically using the density model of Figure 4*b*. The beaded line shows the meridional projection of the DE 1 orbit for the August 17, 1982, case. The outermost dashed line shows the field line located at $L$=5.4. A sharp density gradient at this $L$ shell guides the rays. (*b*) Ducted propagation and subsequent nonducted reflection of 4.1-kHz rays from the northern hemisphere. The duct is located at $L$=3. Total propagation delay is ~1.3 s. This is the mode believed to be associated with the data plotted in the middle of Figure 3*b*.

UT), are also believed to represent ionospheric reflections of initially ducted signals. These points, however, show lower group delays than do the upper points in Figure 3*b*, suggesting that the contributing duct for the third mode may have been at a lower $L$ shell ($L$ ~3) and that reflections may have occurred at lower northern latitudes than in the previous case. One such possible path of propagation is shown in Figure 8*b*, where we have considered a duct located at $L$ ~3 with reflections from the bottom of the ionosphere occurring at ~60°N. For the case shown, the signal is detrapped from the duct at high latitudes and arrives at the ionosphere on higher $L$ shells. The group delays calculated for these rays are within ±10% of the delays for the middle group of data points in Figure 3*b*. Thus while the particular field line of ducted propagation and the point of reflection are not known, the observations are consistent with the mode shown in Figure 8*b*.

The results of the analysis of the data for the August 17, 1982, case further confirm the predominance of two distinct modes of whistler mode wave propagation from a ground source to a high-altitude satellite. These are (1) direct nonducted paths and (2) a hybrid propagation mode involving signals that initially propagate between hemispheres in ducts and that subsequently reflect from the ionosphere up to the satellite locations over a nonducted path. The latter mode of propagation has also been recently identified in cases of magnetospheric signals such as chorus bursts and periodic emissions [*Smith et al.*, 1984]. This may be an important means by which signals amplified and/or generated as a result of wave-particle interactions in magnetospheric ducts can illuminate large portions of the magnetosphere.

## 5. Sidebands and Associated Emissions

The signals received on the DE 1 satellite on August 17, 1982, were associated with sidebands both above and below the Siple transmitter signals. While discussion of the mechanisms of sideband generation is beyond the scope of our paper, we consider how the foregoing propagation mode analysis can be used to obtain information on the ducted or nonducted nature of the signals involved in the sideband generation process. Figure 7 shows the received signals on the satellite together with the transmitted format. The sidebands are clearly visible above and below most of the constant frequency pulses. The measured sideband spacings were ±(30±2 Hz) and are plotted in Figure 9, where the measured spacings for the second- and third-order sidebands are also shown.

Analysis of the sideband amplitudes indicated that sidebands were associated with both the direct (first arriving) signals and the delayed signals arriving ~0.6 s later. A spectrogram of the Siple signal arriving at the satellite at 1740 UT is shown in the top panel of Figure 10, with the later path (labeled B) clearly showing the sidebands. The sec-

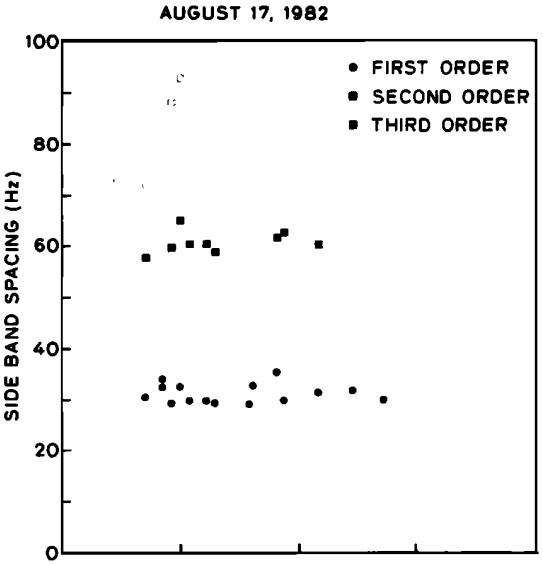


| $\lambda_m$ (deg) | 0 | 1 | 2 | 3 | 4 |
|---|---|---|---|---|---|
| UT | 1735 | 1739 | 1742 | 1746 | 1749 |
| L | 4.54 | 4.51 | 4.49 | 4.46 | 4.43 |
| $\phi_g$ (deg) | -68.52 | -69.52 | -70.27 | -71.27 | -72.15 |

Fig. 9. The sideband spacing measured along the satellite path on August 17, 1982, with different symbols showing the spacings for the first-, second- and third-order sidebands.

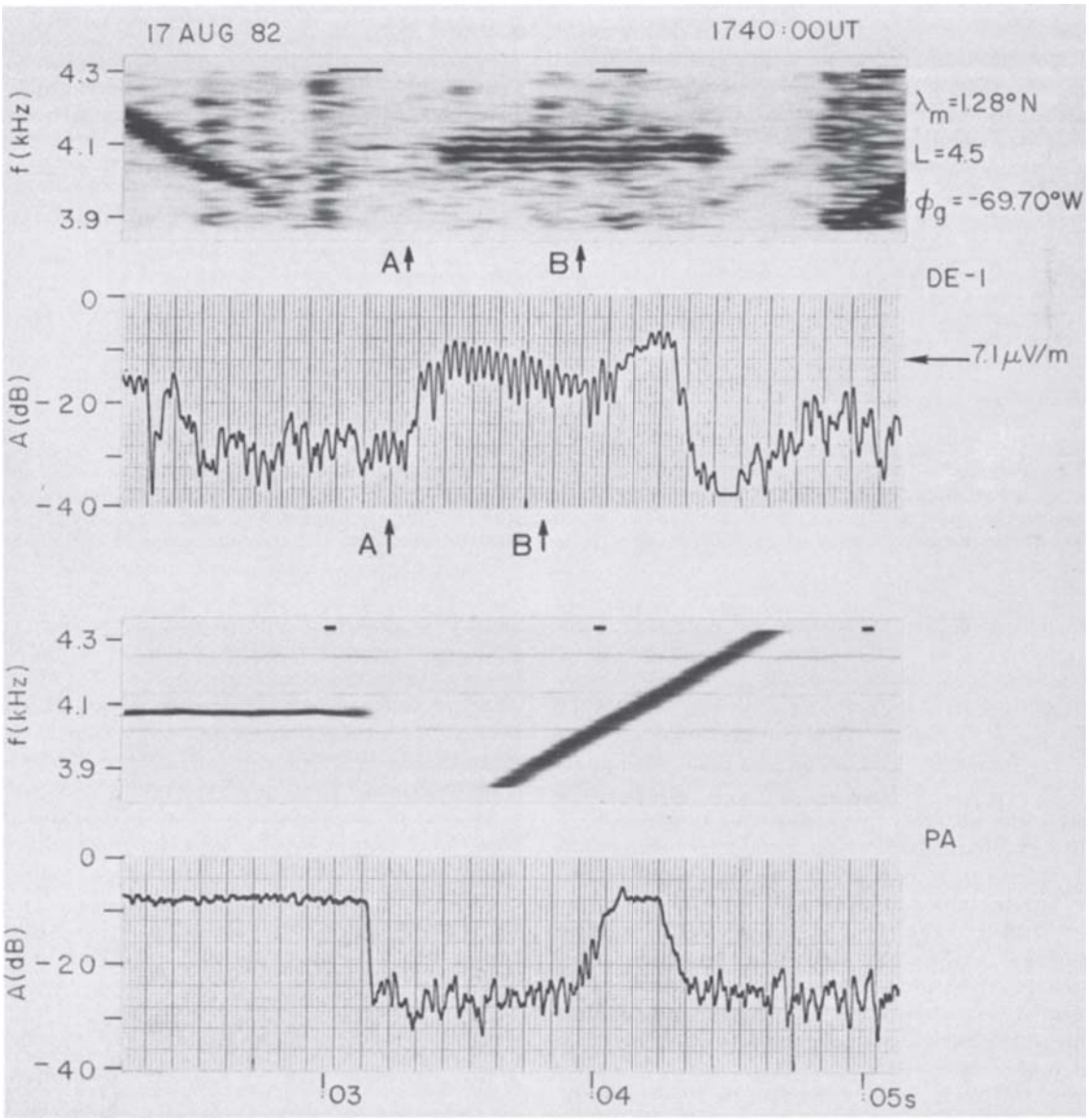


Fig. 10. The top panel shows the spectrogram of Siple signals observed at the DE 1 satellite at 1740 UT on August 17, 1982. The second panel shows the amplitude record of the same signals in a 100-Hz bandwidth (the earlier and later arriving signals are labeled A and B). The amplitude record shows evidence for the same sideband component for the two paths (identified as quasi-regular amplitude modulation). The carrier amplitude for the later path is ~20 dB stronger than for the earlier one. The third panel shows the same signal received at Palmer propagating subionospherically; its amplitude record is shown in the lower panel. The panels are aligned in absolute time.

ond panel of Figure 10 shows the amplitude record of the same signals in a 100-Hz bandwidth filter. The sideband spacing here is indicated by the amplitude modulation period. Although the sidebands on the earlier path (labeled A) are not visible on the spectrogram, the amplitude record clearly shows a quasi-regular amplitude modulation for the first ~ 0.2 s prior to the reception of the later path (labeled B) with the same modulation. Note that the period of the modulation corresponds to ~30 Hz sidebands. The amplitude of the carrier for the later path is ~20 dB higher than the earlier carrier, which accounts for the apparent absence of sidebands on the earlier signals on the spectrograms. The larger carrier amplitude of the later arriving signal can be attributed to possible amplification of the signal along the ducted portion of its path or to ray defocusing on the direct nonducted path.

Sidebands were detected during the period 1736–1836 UT, when the satellite was ~0°–18° north magnetic latitude. The sideband spacing remained constant throughout the ~60 min of detection. The sidebands subsequently became weaker and intermittent as the satellite moved farther north. The sideband structure was first observed when the satellite crossed the equator at 1736 UT, at a time when the receiver was switched from the B to the $E_x$ antenna. If the sideband structure was present at the time of the antenna switch, the fact that it is not observed with the B antenna can be attributed either to the lower sensitivity of the B antenna or to an enhanced E/B ratio for the sidebands. Because the B antenna was used for detection prior to 1736 UT, we cannot determine whether sidebands would have been detected before the satellite crossed the magnetic equator.

The observation of sidebands associated with the trans-

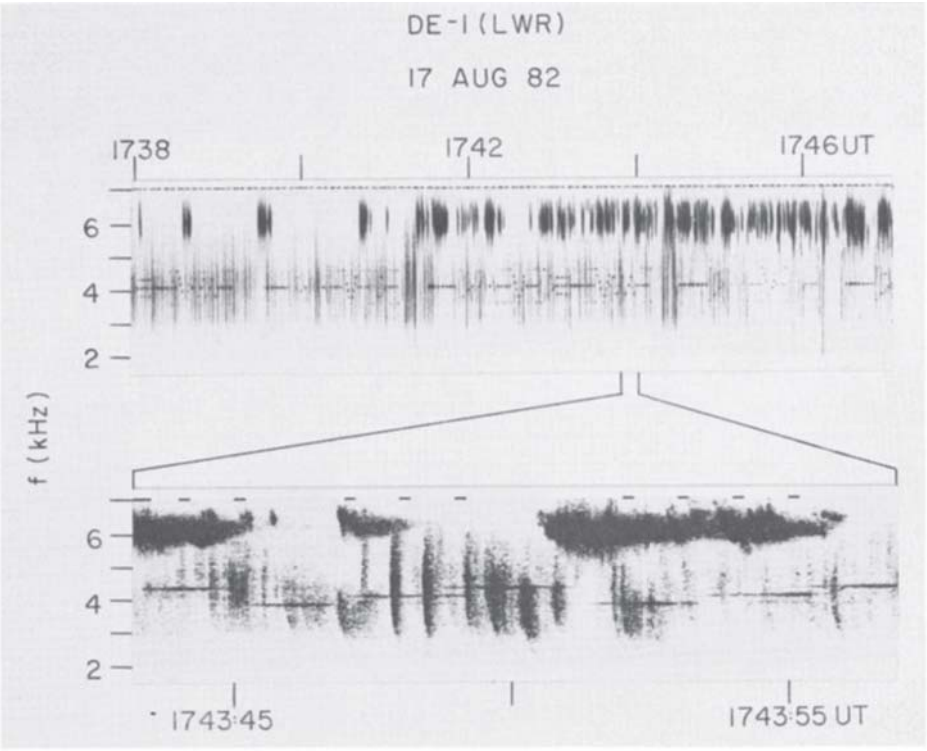


Fig. 11. The top panel shows compressed 2–7 kHz dynamic spectra received on DE 1 (1.5 cm/min) during 1738–1747 UT, showing natural noise bursts and emission activity as well as Siple signals. The lower panel shows a version of the same data near 1743 UT, expanded in time. Both noise bursts and whistlers can be seen.

mitter signal coincided with an active background of natural emission activity. These natural events are shown in Figure 11; the top panel of Figure 11 shows the dynamic spectra received on DE 1 for 1738–1747 UT in a compressed time format while the lower panel shows the time expanded spectra at ~1743 UT. The lower panel shows VLF noise bursts near ~6 kHz, of a type that has been observed on satellites near the plasmapause [*Smith et al.*, 1984] and in ground data has been associated with the precipitation of energetic electrons [*Dingle and Carpenter*, 1981]. These bursts are evidence of conditions suitable for strong wave-particle interactions, which may also be the reason why transmitter signals are associated with sidebands on this particular day. Also observed are pairs of whistler components separated in time delay by ~0.6 s near ~4 kHz, further corroborating the earlier identifications of the first two distinct modes of propagation for Siple signals. The dispersion of the whistlers indicates that the generating lightning flash occurred in the northern hemisphere, while the Siple signals entered the magnetosphere in the southern hemisphere.

Siple signals simultaneously received at Palmer station did not show evidence of sidebands. To demonstrate this, the spectra and amplitude records of Palmer signals are shown in the third and fourth panels of Figure 10 (all panels in this figure are aligned in absolute time).

A more detailed analysis of the sideband spectra are shown in Figure 12 in order to demonstrate the variation in time of the sideband and carrier intensities. The top panel shows a spectrogram of a constant frequency continuous wave signal being received near the time when the receiving antenna was switched from B to E and the sideband activity apparently began. The lower panels show the amplitude scans covering portions of the data marked A through E. The scans cover a 250-Hz band as opposed to 1250 Hz for the spectrogram. These scans are separated by 50 ms, and each scan represents spectra over a period of 8 ms. The filter bandwidth used was 4 Hz. The amplitudes of the sidebands and the carrier vary irregularly; at times the amplitudes of the sidebands are ~10 dB larger than the carrier. These properties and also the lack of dependence of the sideband spacing on the frequency of the carrier signal suggest that the sidebands are not due to interference on board the satellite and/or at the tracking stations but are generated in the medium, presumably by wave-particle interactions.

Ray-tracing analysis conducted with the model of Figure 4*b* suggested that the direct mode signals that showed sidebands (delays plotted as the lower group of data points in Figure 3*b*) propagated in a nonducted mode. The signals also associated with sidebands but arriving 0.6 sec later than the nonducted signals, (delays shown as the middle group of data points of Figure 3*b*) are believed to have propagated in a whistler mode duct along a portion of their path. Similarities in the modulations of these two signals shown in the amplitude record of Figure 10 suggest that the mechanisms generating the sidebands may have been similar for both the direct nonducted and the reflected rays. Siple signals during this period were also on occasion seen to trigger rising emissions (Figure 7). The triggering of these risers is further evidence that the sidebands resulted from interactions with energetic particles.

In many ways, the characteristics of the observed sidebands are similar to those observed in association with ducted Siple signals observed on the ground [*Park*, 1981]. The sidebands are an indication of nonlinear wave-particle

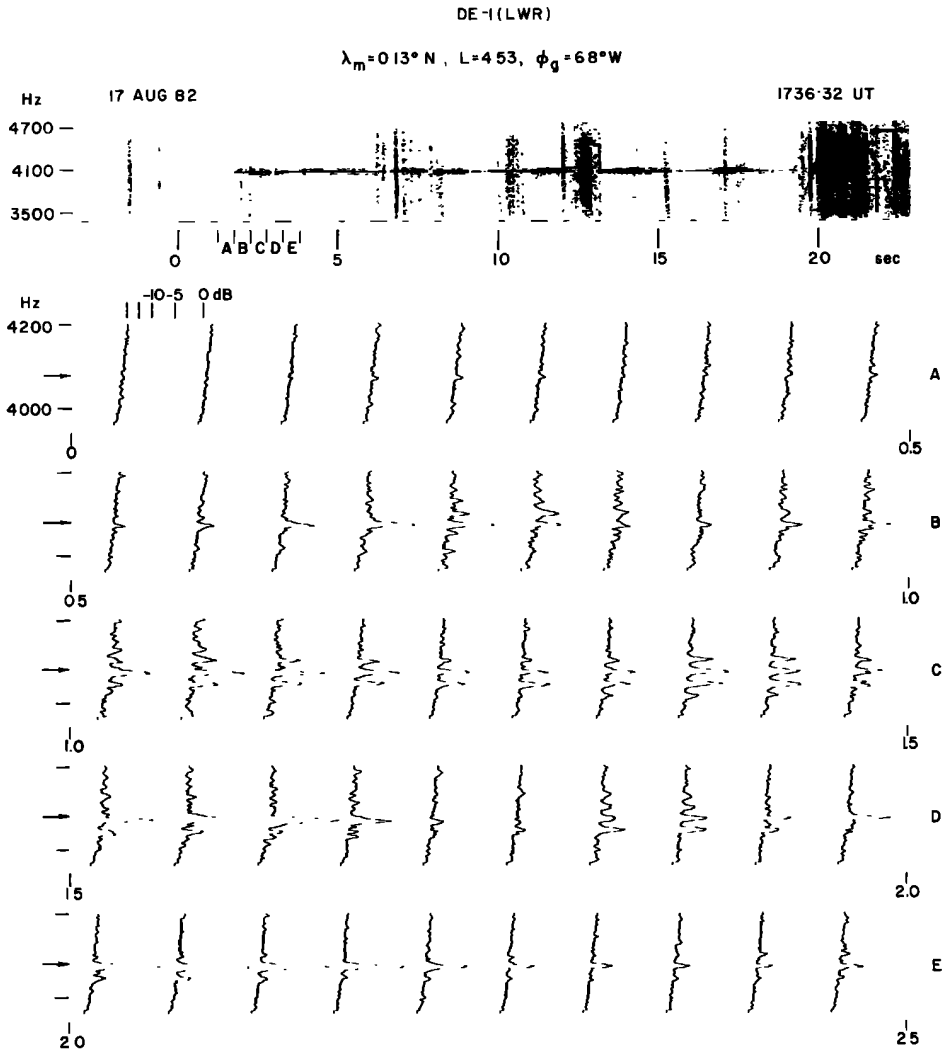


Fig. 12. The top panel shows the spectrogram of the CW signal received at the satellite during the time that the receiving antenna was switched from B to E. The lower panels are the amplitude scans of the segments A through E marked on the top panel. The scans cover a 250-Hz band as opposed to 1250 Hz for the spectrogram. These scans are separated by 50 ms and each scan represents spectra over a period of 8 ms. The filter bandwidth used was 4 Hz.

interactions between the Siple signals and the energetic electrons. The analysis of the propagation paths indicates that at least one of the two signals arriving at the satellite propagated in a nonducted mode. This observation may be the first reported case of sidebands associated with nonducted waves.

Our discussion of the August 17, 1982, sidebands has been limited to those aspects which can be deduced from propagation mode analysis. The results presented raise new questions concerning the location of the sideband generation region. The discussion above indicates that the direct ray arriving at the satellite after traversing the equator shows relatively weak sideands, while the reflected ray is largely amplified even though it has also crossed the equator. This may a result of the presumption that the latter has crossed the equator while propagating in the ducted mode. Recent experimental and theoretical work has indicated that the threshold of signal intensity for generation of nonlinear effects may be somewhat higher for nonducted signals [*Bell et al.*, 1981; *Bell*, 1984]. Thus the signal propagating in the ducted mode may be amplified while the direct signal is not. Further work beyond the scope of this paper is required in order to understand better the nature of the sideband generation mechanisms.

## 6. Summary and Discussion

We have presented detailed analysis of two selected cases of reception of Siple transmitter signals on the Dynamics Explorer 1 satellite. Direct measurements of the wave magnetic and electric field intensities provided values that are consistent with past observations (see the appendix). The analysis of VLF ray propagation paths to the satellite revealed the presence of direct paths and ionospherically reflected paths on both days. The reflected (or hybrid) mode usually involved ducted propagation from the transmitter in the south to the conjugate point in the north and subsequent reflection from the top of the ionosphere. The spatial and temporal extent of the DE 1 observations of this hybrid mode indicates that it may be an important means by

which signals amplified or triggered in ducts may illuminate relatively large magnetospheric regions.

An equatorial cold plasma density distribution was constructed using data from the in situ density measurements, ground-based whistler measurements, and an assumed diffusive equilibrium model. Comparison of measured group delays with those computed from ray tracing provide quantitative determination of raypaths. The group delays computed based on the diffusive equilibrium model and in situ densities were found to be in good agreement with the measured delays over a wide range of magnetic latitudes (50°S–25°N). This finding is evidence of the validity of the use of the diffusive equilibrium model to describe the distribution of cold plasma along the magnetic field lines.

In one of the cases studied Siple signals at various frequencies were seen to be associated with sidebands having ±30 Hz spacing. Sidebands of similar spacing were found to be present on signals arriving over different paths. The later arriving signals were also seen to occasionally trigger emissions. Ray path analysis provided information on what we believe to be the first identification of sidebands generated as a result of wave-particle interactions involving nonducted waves.

## 7. Appendix: Wave Signal Intensity and Refractive Index

In this appendix we discuss briefly the measurement of wave signal intensities for the two cases studied.

Absolute magnetic and electric field intensities of Siple signals observed on DE 1 were measured using a filter bandwidth of 100 Hz around the transmitter frequency. The receiver for May 24, 1982, was connected to the loop (B) antenna and the measured values in picoteslas are shown in Figure 13*a*. Most of the data on August 17, 1982, were acquired with the electric ($E_x$) antenna, with a few brief receptions in the B antenna mode. The measured electric field for this case is shown in Figure 13*b*. The measured B field intensities during the short period of 1735–1736 UT were in the range 0.03–0.07 pT.

In order to compare the measured wave intensities for May 24, 1982, with previously reported measurements of Siple signals on the IMP 6 satellite on June 28, 1973 [*Inan et al.*, 1977], we selected an orbital location common to both days at which time DE 1 was at a geographic longitude of ~66°W and $L$ ~4.5. The distance from the Siple transmitter to the foot of the field line was found to be ~680 km. A simple model of the subionospheric propagation losses with nighttime ionospheric $D$ region absorption of ~5 dB (including 3 dB polarization loss) at 4.6 kHz [*Helliwell*, 1965] yields an expected power density at the satellite location of $\sim 8\times10^{-15}$ W/m$^2$. This takes into account the divergence of the illuminating ray paths (shown earlier for the May 24, 1982, case), causing the wave power density to decrease along the ray path. The local refractive index was estimated from raytracing analysis to be ~30 for longitudinal propagation and ~31 for a wave normal angle ~18°. Using the wave power density in conjunction with this refractive index value yields wave magnetic field intensity of ~0.03 pT for field aligned propagation. Data of Figure 5 show a measured wave intensity of ~0.056 pT at ~2300 UT, which is in reasonable agreement with the estimated value of ~ 0.03 pT.

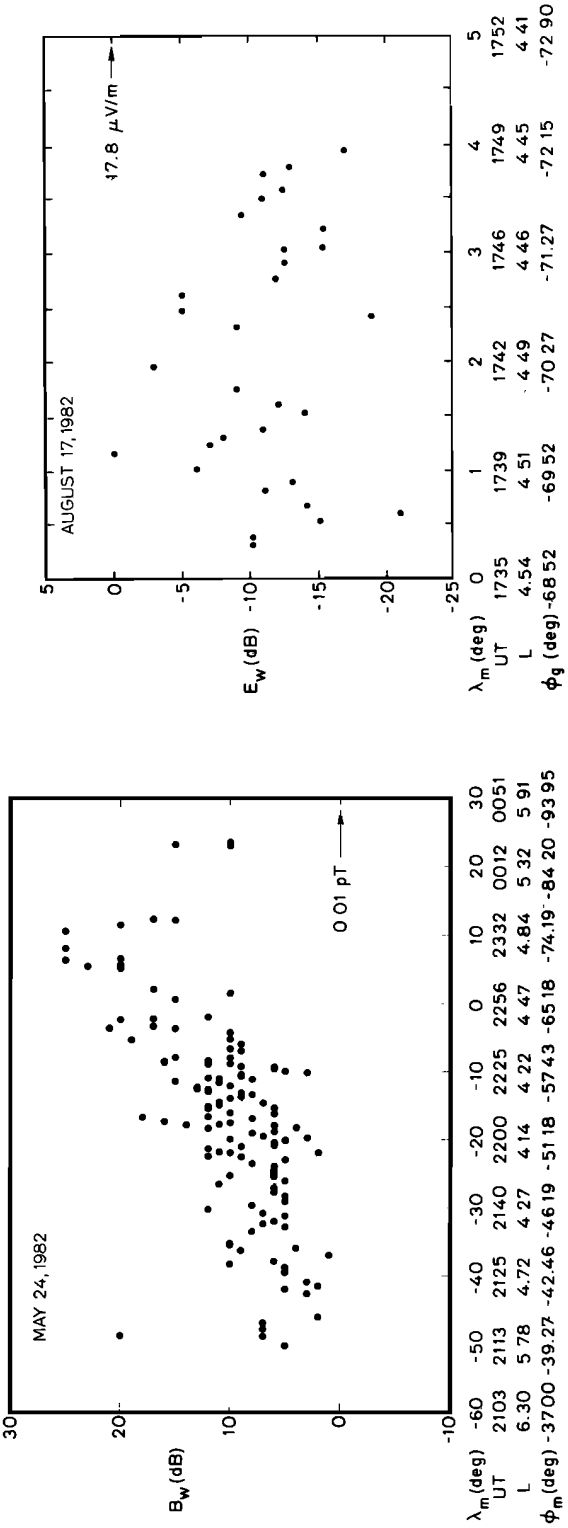


Fig. 13. (*a*) Magnetic field intensities of the Siple signal measured on DE 1 during 2113–0020 UT on May 24, 1982; 0 dB corresponding to 0.01 pT. (*b*) Electric field intensities of the Siple signal measured aboard the satellite during 1735–1750 UT on August 17, 1982, with 0 dB corresponding to 17.8 μV/m.

Following the same procedure as given above, in the IMP 6 case of June 28, 1973, the distance from the transmitter to the foot of the field line located at L~3.84 was estimated to be ~910 km. The estimated power density at the location of the satellite is $\sim 8.0 \times 10^{-11}$ W/m$^2$ using an estimated ionospheric absorption of ~5 dB at 5 kHz. The local refractive index at the location of the satellite was ~8 [*Inan et al.*, 1977] which along with the power density yields a wave intensity of ~1.6 pT. This value is to be compared with the measured value of 0.3 pT for that case [*Inan et al.*, 1977].

It is interesting to note that both the estimated and measured values for June 28, 1973 (IMP 6), are larger than those for May 24, 1982 (DE 1), due to the difference in ray path distributions (i.e., background cold plasma distribution) for the two days, resulting in significantly less defocusing of rays for the former.

*Acknowledgments.* We appreciate discussions with our colleagues in the STAR laboratory of Stanford University. We specifically acknowledge the contributions of J. P. Katsufrakis in directing the field operations at Siple and Roberval stations and in helping to set up the DE 1/Siple real time experiments. We thank J. Yarbrough for generating the spectrograms and charts used for analysis and presentation. The SFR data were provided through the courtesy of S. D. Shawhan and D. A. Gurnett of University of Iowa. We thank J. Green of Marshall Space Flight Center for processing the SFR data and providing the derived in situ plasma densities. This work was supported by the National Aeronautics and Space Administration under contract NAS5-25688. The Siple, Roberval, and Palmer Station experiments are supported by the Division of Polar Programs of the National Science Foundation under contracts DPP-83-17092,DPP-83-18508 and DPP-82-17820. The typescript was prepared by N. Leger.

The Editor thanks T. Neubert and another referee for their assistance in evaluating this paper.

## REFERENCES

Angerami, J. J., and J. O.Thomas, Studies of planetary atmospheres, 1, The distribution of electrons and ions in the earth's exosphere, *J. Geophys. Res.*, *69*, 4537, 1964.

Bell, T. F., The nonlinear gyroresonance interaction between energetic electrons and coherent VLF waves propagating at an arbitrary angle with respect to the earth's magnetic field, *J. Geophys. Res.*, *89*, 905, 1984.

Bell, T. F., U. S. Inan and R. A. Helliwell, Nonducted VLF waves and associated triggered emissions observed on the ISEE 1 satellite, *J. Geophys. Res.*, *86*, 4649, 1981.

Bell, T F., R. A. Helliwell, U. S. Inan, I. Kimura, H. Matsumoto, T. Mukai, and K. Hashimoto, EXOS-B/Siple station VLF wave-particle interaction experiments: 2, Transmitter signals and associated emissions, *J. Geophys. Res.*, *88*, 295, 1983.

Burtis, J. W., User's guide to the Stanford VLF raytracing program, technical report, Radiosci. Lab., Stanford Electr. Lab., Stanford, Calif., 1973.

Carpenter, D. L., R. R. Anderson, T. F. Bell, and T. R. Miller, A comparison of equatorial electron densities measured by whistlers and by a satellite radio techniques, *J. Geophys. Res.*, *86*, 1107, 1981.

Dingle, B., and D. L. Carpenter, Electron precipitation induced by VLF noise bursts at the plasmapause and detected at conjugate ground stations, *J. Geophys. Res.*, *86*, 4597, 1981.

Gorney, D. J., and R. M. Thorne, A comparative ray-trace study of whistler ducting processes in the earth's plasmasphere, *Geophys. Res. Lett.*, *72*, 133, 1980.

Helliwell, R. A., *Whistlers and Related Ionospheric Phenomena*, Stanford University Press, Stanford, Calif., 1965.

Inan, U. S., and T. F. Bell, The plasmapause as a VLF wave guide, *J. Geophys. Res.*, *82*, 2819, 1977.

Inan, U. S. and R. A. Helliwell, DE 1 observations of VLF transmitter signals and wave-particle interactions in the magnetosphere, *Geophys. Res. Lett.*, *9*, 917, 1982.

Inan, U. S., T. F. Bell, D. L. Carpenter, and R. R. Anderson, Explorer 45 and IMP 6 observations in the magnetosphere of injected waves from the Siple station VLF transmitter, *J. Geophys. Res.*, *82*, 1177, 1977.

Inan, U. S., R. A. Helliwell, and J. P. Katsufrakis, DE 1 observations of Siple transmitter signals and triggered and natural VLF emissions near the geomagnetic equator, *EOS Trans. AGU*, *63*, 45, 1982.

Moiser, S. R., M. L. Kaiser, and L. W. Brown, Observations of noise bands associated with the upper hybrid resonance by the IMP 6 radio astronomy experiment, *J. Geophys. Res.*, *78*, 1673, 1973.

Park, C. G., Methods of determining electron concentrations in the magnetosphere from nose whistlers, *Tech. Rep. 3454-1*, Radiosci. Lab., Stanford Electr. Lab., Stanford, Calif., 1972.

Park, C. G., Generation of whistler mode sidebands in the magnetosphere, *J. Geophys. Res.*, *86*, 2286, 1981.

Persoon, A. M., D. A. Gurnett and S. D. Shawhan, Polar cap electron densities from the DE 1 plasma wave instrument, *J. Geophys. Res.*, *88*, 10123, 1983.

Shawhan, S. D., A. G. Donald, L. O. Daniel, R. A. Helliwell, and C. G. Park, The plasma wave and quasi-static electric field instrument (PWI) for Dynamics Explorer A, in *Dynamics Explorer*, edited by R. A. Hoffman, p. 535, D. Reidel, Hingham, Mass., 1981.

Smith, A. J., D. L. Carpenter and U. S. Inan, Whistler triggered VLF noise bursts observed on the DE 1 satellite and simultaneously at Antarctic ground stations, *Ann. Geophys.*, in press, 1985.

R. A. Helliwell, U. S. Inan, and K. Rastani, Space, Telecommunications, and Radioscience Laboratory, Stanford University, Stanford, CA 94305.

(Received July 6, 1984;
revised December 3, 1984;
accepted December 10, 1984.)